Electronic Supplementary Material (ESI) for Journal of Materials Chemistry A.


# Supplementary material: Correlating light-induced deep defects and phase segregation in mixed-halide perovskites

Katarína Ridzoňová [*a,d], Roman Grill [d], Amalraj Peter Amalathas [b,e], Branislav Dzurňák [b], Neda Neykova [a,b], Lukáš Horák [d], Peter Fiala [c], Xin Yu Chin [c], Christian M. Wolff [c], Quentin Jeangros [c] and Jakub Holovský [a,b]

[a] Institute of Physics, Czech Academy of Sciences, Cukrovarnická 10, 16200 Prague, Czech Republic

[b] Centre for Advanced Photovoltaics, Faculty of Electrical Engineering, Czech Technical University in Prague, Technická 2, 16627 Prague, Czech Republic

[c] Institute of Electrical and Microengineering (IEM), Photovoltaic and Thin-Film Electronics Laboratory, École Polytechnique Fédérale de Lausanne (EPFL), Rue de la Maladière 71b, 2002 Neuchâtel, Switzerland

[d] Faculty of Mathematics and Physics, Charles University, Ke Karlovu 5, 121 16, Prague, Czech Republic

[e] Department of Physics, Faculty of Science, University of Jaffna, Jaffna 40000, Sri Lanka

* Correspondence: ridzonova@fzu.cz

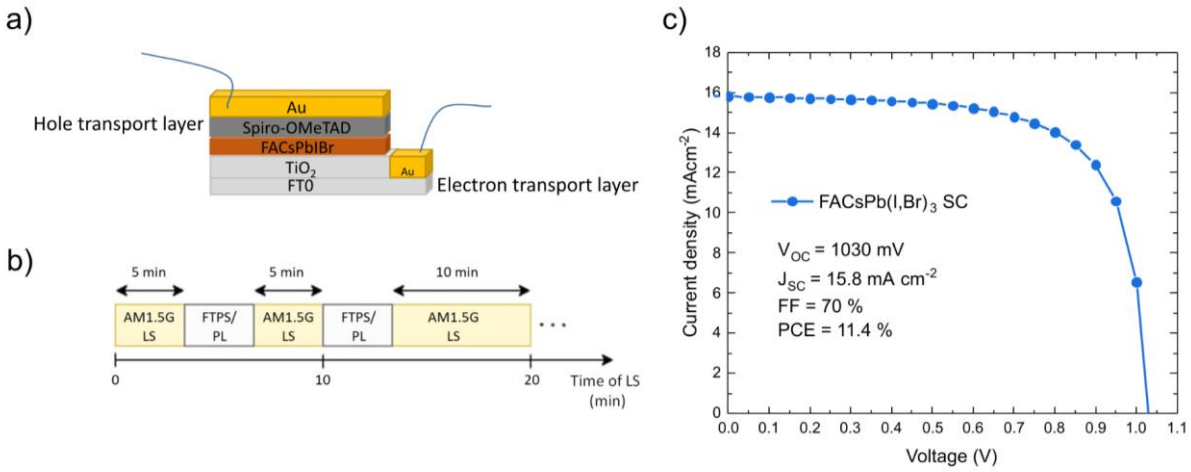


Fig. S1: a) Scheme of studied solar cell device, b) scheme of measurement sequence, c) *J-V* data measured on $FA_{0.83}Cs_{0.17}Pb(I_{0.6}Br_{0.4})_3$ solar cell together with photovoltaic parameters.

## 1. PL measurements

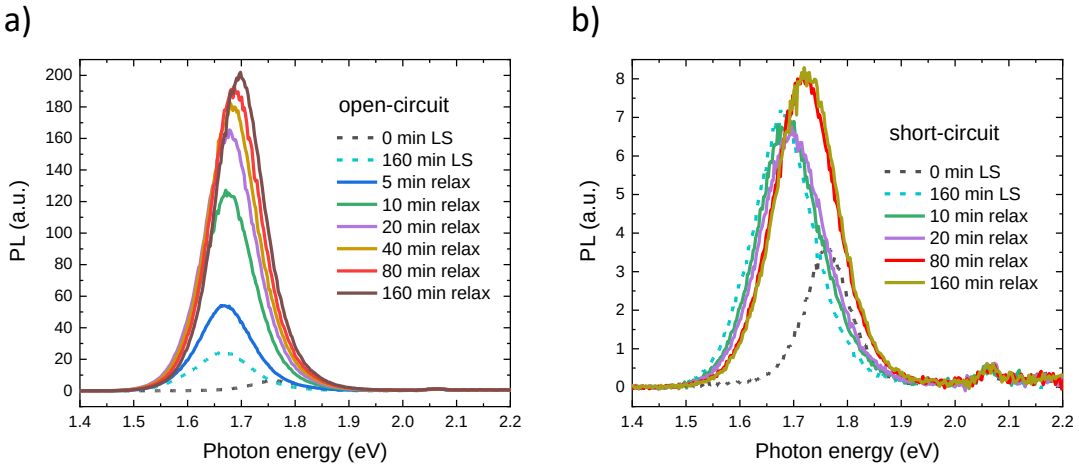


Fig. S2: Time evolution of photoluminescence spectra measurements during relaxation in the dark at a) open-circuit and b) short-circuit conditions.

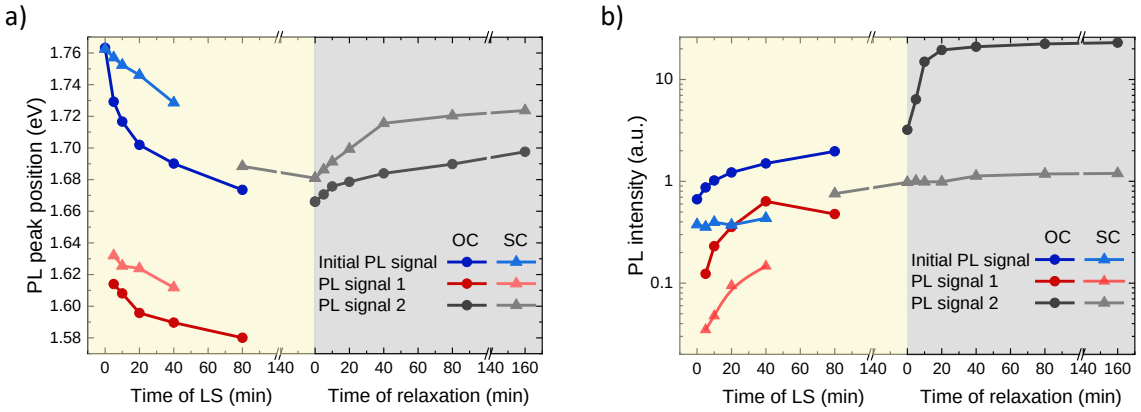


Fig. S3: The evolution of a) PL peak positions and b) integrated PL intensities of the initial high bandgap peak and newly formed peaks 1 and 2 during LS and relaxation in the dark.

## 2. FTPS measurements

### 2.1. $I_2$/ $PbI_2$ formation

A distinct feature at 2.5 eV appears during LS in the above-bandgap part of the FTPS spectra at OC and MPP condition (see Fig. 7a and S5). This feature can be assigned to the $I_2$/$PbI_2$ formation what is in good accordance with spectra measurements in [1]. Connection of this feature with iodine may also explain spectra measurements on mixed-halide perovskites with varying *I* and *Br* concentration from x= 0 to x= 1 in Ref. [2]. Here increasing iodine concentration lead to a more pronounced hump at 2.5 eV and is completely missing in case of pure $MAPbBr_3$ perovskites. $PbI_2$ formation is supported by previous formation of an $I_2$ molecule [3]. Electron trapping at the positively charged $I_i^+$ or hole trapping at the negatively charged $I_i^-$ and subsequent reaction of two filled traps $I_i^0$ can lead to formation of an $I_2$ molecule which tends to migrate to the surface [3]. Iodine imbalance between surface and bulk can trigger series of compensating reactions and as a consequence $PbI_2$ may segregate as a separate phase [3]. Such formation mechanism explains why feature at 2.5 eV is not visible in case of samples light-soaked at short-circuit. Phenomenon is observed only at open-circuit and MPP condition when the higher concentration of light induced iodine interstitials and photo-generated carriers encourages $I_2$ and subsequent $PbI_2$ formation.

### 2.2. Drop (increase) in the deep defect concentration at longer times of LS (after switching off LS)

The observed drop in the concentration of deep level defects at longer times of LS (Fig. 3a-160 min) may be explained by the formation of $I_2$/$PbI_2$ from iodine interstitials. This explanation is consistent with the fact that the decrease in deep defect concentration occurs only in those samples where after a long period of LS a considerable feature at 2.5 eV emerges. The initial increase in defect concentration in the case of OC within first 5 min of relaxation is probably also related with $I_2$ molecules. After switching off the illumination, there is an excess concentration of light-generated vacancies which may react with an $I_2$ molecule and lead to its decay. During the decay of an $I_2$ molecule, one iodine occupies the vacancy and the second iodine remains in the sample as an interstitial. Therefore, we observe such a sudden increase in iodine interstitial concentration during first minutes of relaxation in dark. Such mechanism of initial increase in defect concentration during relaxation due to decay of an $I_2$ molecule correlates well with the observation that steep increase is pronounced more, the larger the hump at 2.5 eV is and that it is completely missing at SC when the hump at 2.5 eV is not observed.

Another possible explanation of the drop in the deep defect concentration at longer times of LS is that phase 2 may cause the formation of a barrier which is less permeable to vacancies. As a consequence, $V_I$ accumulate in the grain interior and recombine more with the new light-induced iodide interstitials. Such explanation is consistent with the observation that drop in deep defect concentration at longer times of LS is observed only when phase 2 occurs and may explain also the sudden increase in the deep defect concentration after switching off the illumination. As the new Frenkel pairs are no longer formed without a source, the previously formed $V_I$ quickly recombine with $I_i$ diffusing from the surface. Other interstitials then have nothing to recombine with, what leads to the increase in their concentration. Since phase 2 makes up 10% of the material, the formation of a diffusion barrier is well justified.

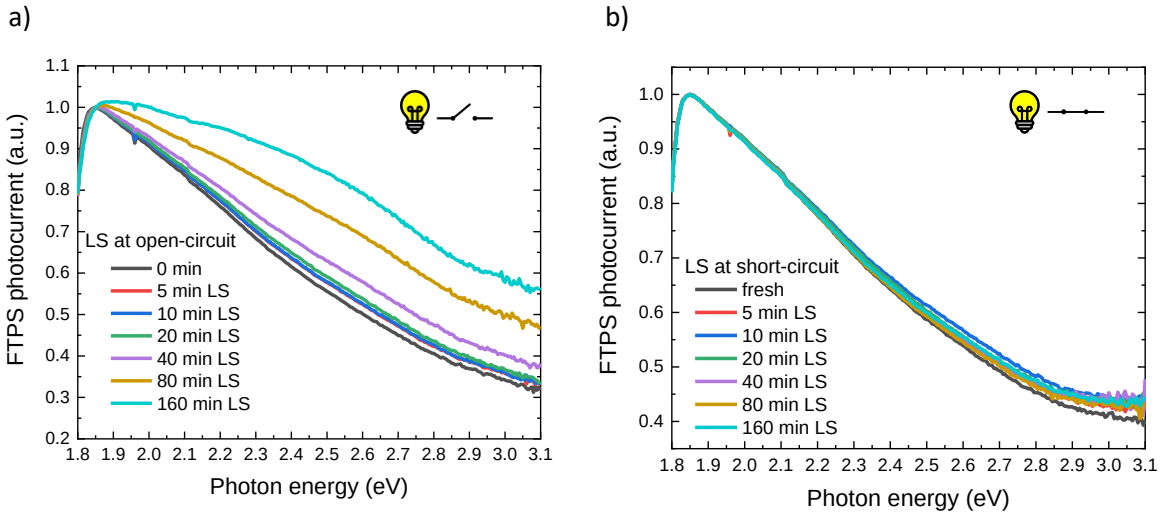


Fig. S4: Evolution of above-bandgap FTPS spectra during LS at a) OC, b) SC.

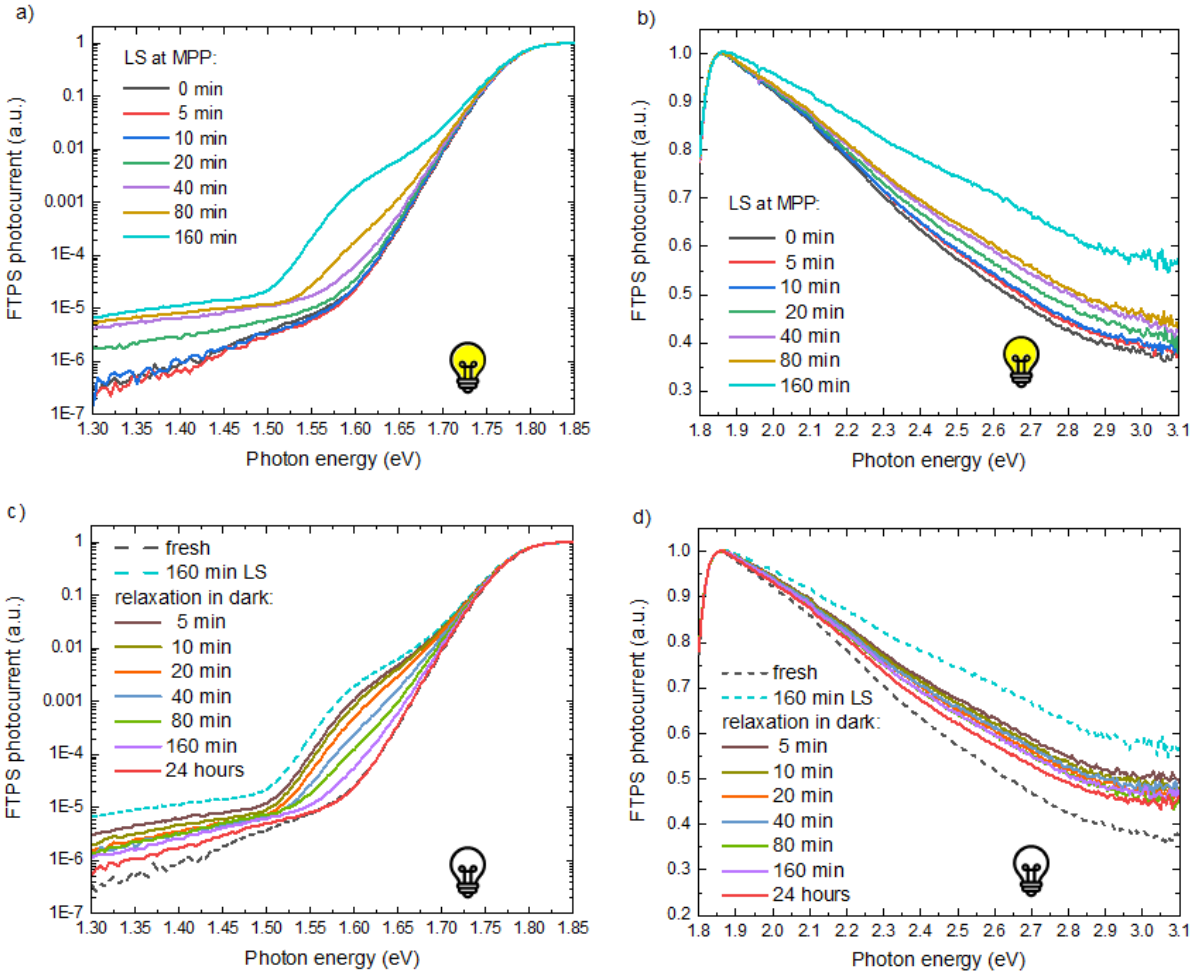


Fig. S5: Fourier-transform photocurrent spectra showing the effect of continuous AM1.5G illumination measured under MPP tracking (top panels) and subsequent relaxation in dark (bottom panels). Spectra are divided into the region of a), c) the sub-bandgap absorption which is illustrated in logarithmic scale and into the b), d) region of above-bandgap absorption in linear scale.

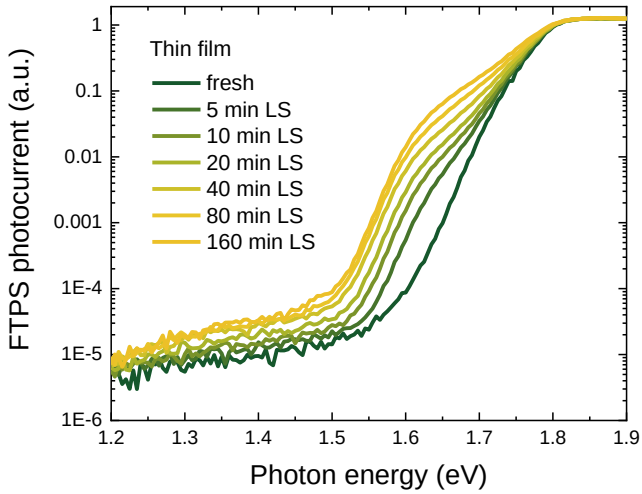


Fig. S6: Evolution of FTPS measured on thin films under continuous AM1.5G illumination. Spectra were measured under applied voltage 100 V.

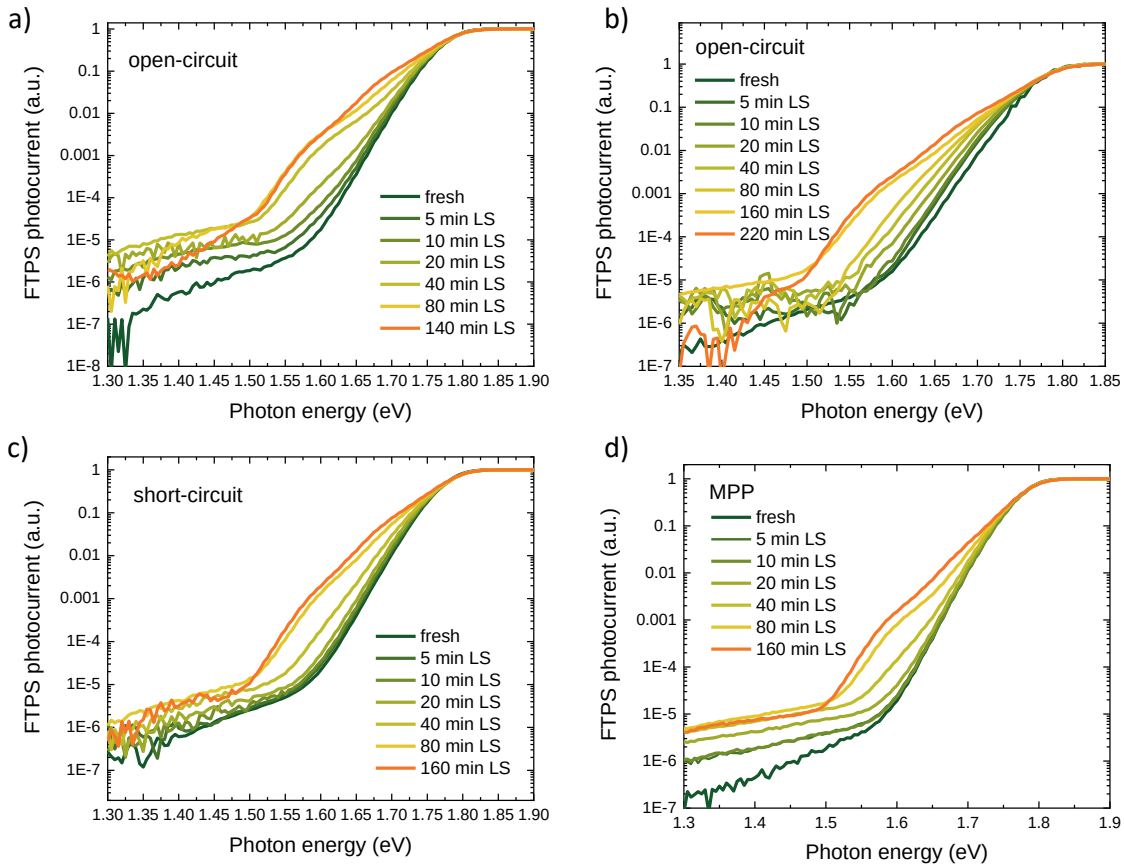


Fig. S7: a)-d) additional FTPS measurements measured on multiple $FA_{0.83}Cs_{0.17}Pb(I_{0.6}Br_{0.4})_3$ solar cells confirming the repeatability of the sub-bandgap signal decrease at longer times of LS, which is accompanied by the formation of the phase 2 with x=0.8.

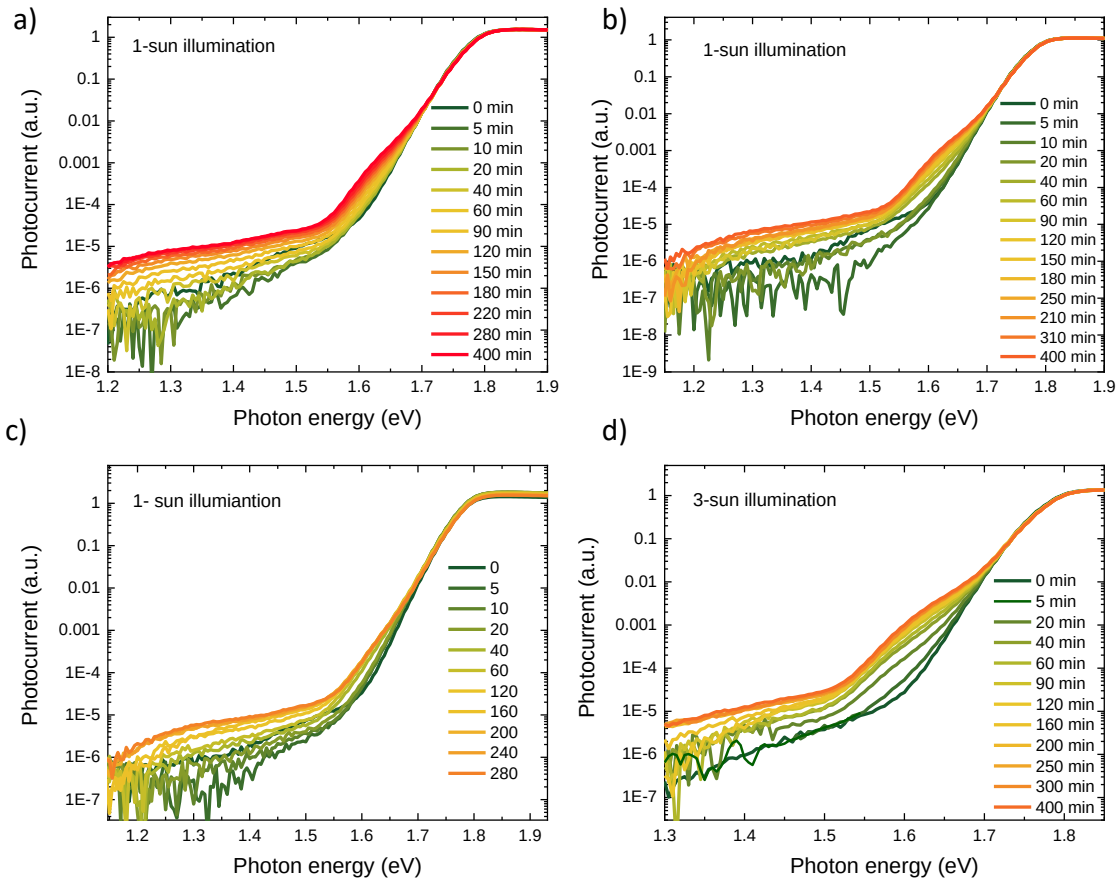


Fig. S8: a)-d) additional FTPS measurements measured on multiple $FA_{0.83}Cs_{0.17}Pb(I_{0.6}Br_{0.4})_3$ solar cells where phase 2 is not formed even under a long-term illumination.

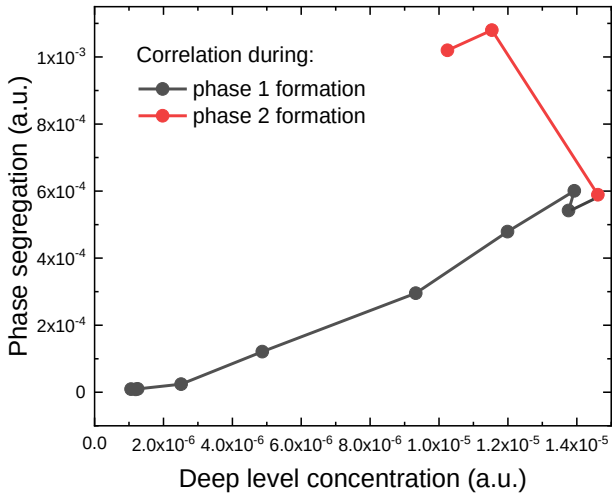


Fig. S9: Correlation of deep level concentration (given by the photocurrent at 1.45 eV) and phase segregation (given by the photocurrent at 1.58 eV). Measured on sample where phase 2 is formed under a long-term illumination.

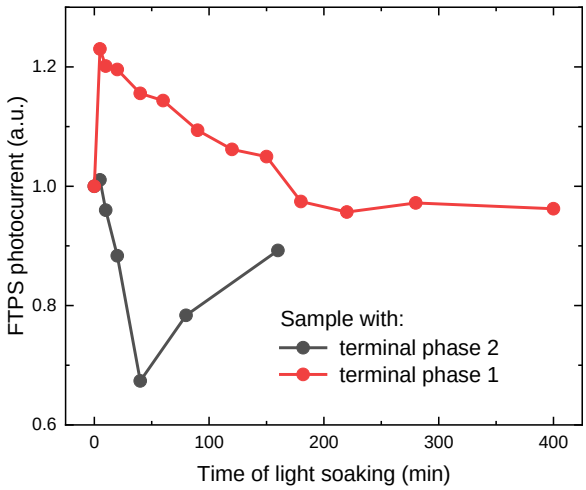


Fig. S10: Comparison of typical evolution of photocurrent signal, obtained at fixed photon energy 1.85 eV from non-normalised FTPS spectra, for samples with terminal phase 1 and 2.

## 3. X-ray diffraction data

We have measured X-ray diffraction (XRD) powder pattern of perovskite layer in pristine state and irradiated for 5, 20 and 40 minutes to support the existence of phase segregation under LS. Thanks to the dependency of lattice parameter on the halide content [4, 5], the phase separation into I-rich and Br-rich regions should be observable in the XRD pattern as the splitting or appearance of new diffraction peaks. Such light-induced peak splitting was reported in $MAPb(I,Br)_3$ by Hoke et al. [2] and Hu et al. [6].

The measured diffraction pattern of $FA_{0.83}Cs_{0.17}Pb(I_{0.6}Br_{0.4})_3$ thin film in Fig. S11 corresponds to the cubic perovskite phase of claimed composition, in accordance with [7, 8]. As seen in Fig. S11b, with a longer light soaking the peak (200) starts to be strongly asymmetric, being composed seemingly of two peaks. The original peak is slightly shifting towards higher diffraction angles and gets wider, while the new less intense peak is located at lower diffraction angles. Not so pronounced, but similar behaviour can be observed for peak (111) (Fig. S11c). When segregation occurs, the I-rich and Br-rich regions should have larger and smaller lattice parameters, respectively, compared with the well mixed homogeneous phase [5]. The observed splitting to lower diffraction angles may be therefore associated with the formation of I-rich phase, while shift to higher diffraction angles with Br-rich phase. Comparing the cubic (200) reflections for $FA_{0.83}Cs_{0.17}Pb(I_{1-x}Br_x)_3$ perovskites with varying Br composition, the light-induced peak at ~ 28.6° corresponds best to the cubic (200) reflection of $FA_{0.83}Cs_{0.17}Pb(I_{0.75}Br_{0.25})_3$, which is close to the estimated composition ($I_{0.8}Br_{0.2}$) of phase 2 observed in PL and FTPS spectra (Fig. 2, Fig. 3, Fig. S7). Regarding the phase 1, observed in PL and FTPS spectra, it is expected that its contribution to XRD pattern must be below the detection limit of XRD, thanks to the low concentration of segregated phase 1 (~ 0.1%).

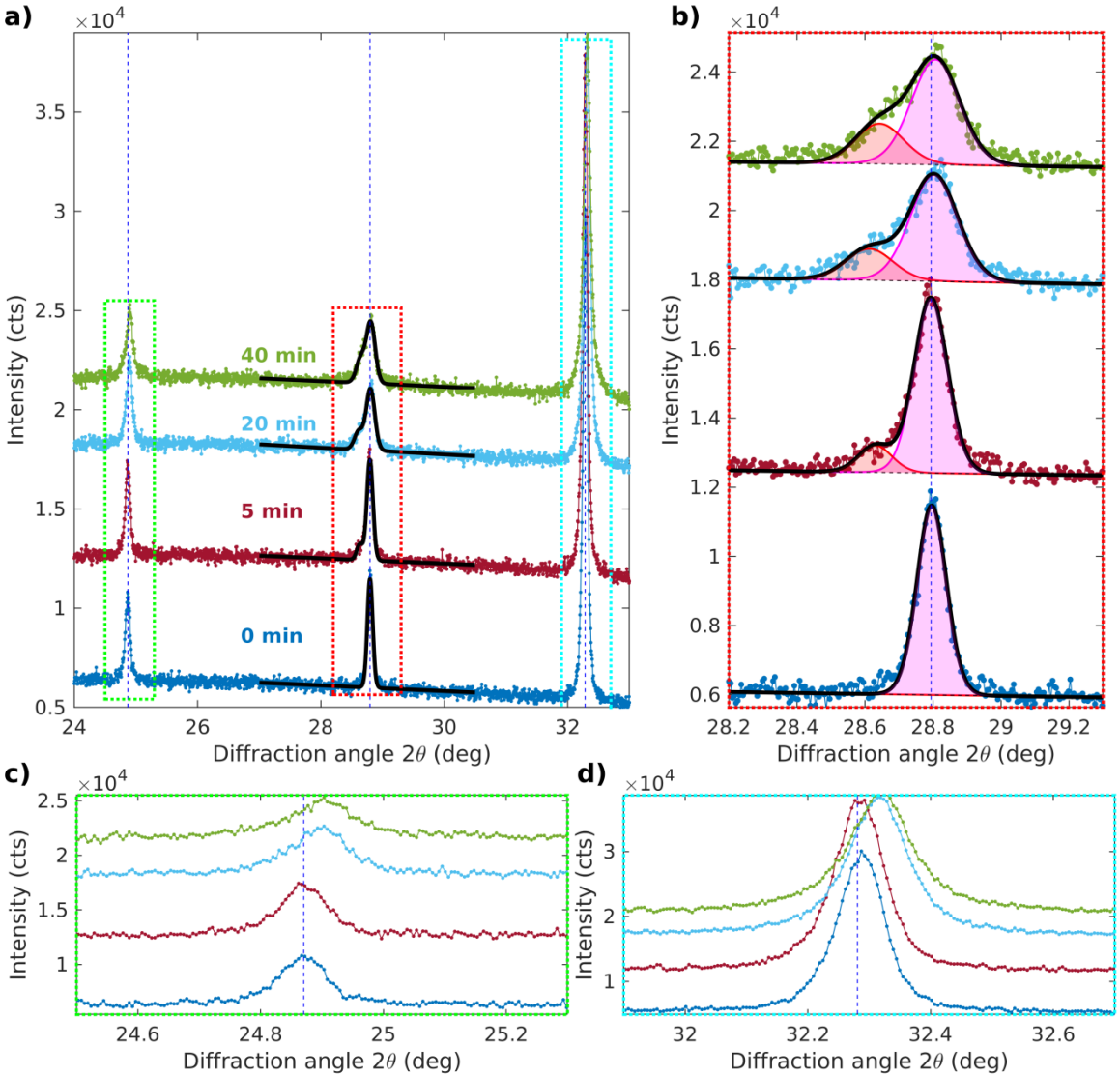


Fig. S11: XRD powder patterns showing the effect of a continuous AM1.5G illumination on a thin film $FA_{0.83}Cs_{0.17}Pb(I_{0.6}Br_{0.4})_3$. a) Cubic peaks (111), (200) and (201) at diffraction angles 24.87, 28.8, and 32.8 deg are shown, respectively. A detail of b) (200), c) (111) and d) (201) XRD peak.

Interestingly, peak (201), shown in Fig. S11d does not exhibit any visible splitting, only becomes wider and shifted to higher diffraction angles. If all of these phases were cubic and homogenous, we should observe the splitting of all the peaks in the diffraction pattern similar to Hoke's measurement [2]. On the contrary, we assume that firstly an I-rich non-homogenous layer is formed under LS in the close vicinity of grain boundaries of 220 nm large grains, as shown in Fig. 6b. This picture is consistent with the model of Br-rich/I-rich core-shell particles with a large amount of defects. Therefore we expect to observe broadening and asymmetry of the peaks rather than splitting. The diffraction pattern should be calculated using Debye formula taking into account strain field resulting from different composition between core and shell. Since sample degradation in the ambient air forced us to collect data in very limited time, the data are not sufficient for unambiguous line profile analysis. Nevertheless, qualitatively we observe the *hkl*-dependent splitting, broadening and shift of the peaks as we expected for such core-shell system. On the basis of these indications,

we are quite convinced that phase segregation to I-rich and Br-rich regions actually occurs in our sample during light soaking.

## 4. Numerical estimations regarding the phase 1 and 2

Using the molecular weight MW of 1 mol of $FA_{0.83}Cs_{0.17}Pb(I_{0.6}Br_{0.4})_3$ (591 $g.mol^{-1}$) obtained from particular atomic masses, the Avogadro constant *A* ($6.022 \cdot 10^{22}$ $mol^{-1}$), the mass density $\rho$ of lead halide perovskite $CH_3NH_3PbI_3$ (3950 $kgm^{-3}$) and average grain size obtained from SEM measurement (2R=220 nm), one can estimate the number of molecules *N* in one grain as:

$$N = \frac{4}{3}\pi R^3 \rho \frac{A}{MW}. \tag{S1}$$

The number of iodine atoms in one grain can be then obtained by multiplying the number of molecules *N* by an iodine stoichiometry factor 0.6x3. Considering that phase 1 makes up according to the FTPS measurement 0.1 % of perovskite at 160 min of LS, we estimate that 40 000 iodine interstitials participate on formation of phase 1. Such amount of iodine atoms is not sufficient to cover whole grain boundary by well resolved new phase 1. We thus expect that iodine atoms further diffuse along the grain boundary and concentrate at seeds convenient for the new phase nucleation, typically the interface of more than two grains.

## 5. Diffusion equation in a sphere

To outline the dependence of phase segregation velocity on the grain size, we solve the diffusion equation for the transport of light-induced $I_i$ in a spherical grain of radius R. The diffusion coefficient $D_i$ of $\sim 2\times10^{-9}$ $cm^2s^{-1}$ [9,10] and average grain size of $\sim$ 220 nm enable fast diffusion of $I_i$ toward the grain surface within $\sim$ 50 ms. Considering that the transport of defects is mediated purely by the diffusion and taking into account that photo-excited defects recombine at the grain boundary in the time range of ~50 ms, which is much less than the characteristic time used at the measurement (tens of minutes), we may neglect the time derivative at the diffusion equation and express the diffusion in the quasi-steady-state approximation as

$$0 = \frac{\partial C_i}{\partial t} = G + D_i \Delta C_i, \tag{S2}$$

where the time derivative can be neglected. Here, $C_i$ represents the deep defect concentration of $I_i$ created at a constant generation rate G per unit volume per second and $D_i$ stands for the diffusion constant of $I_i$. The same equation applies to the diffusion of iodine vacancies. After rewriting eq. S2 in a spherical coordinates and considering no angular dependence of the concentration $C_i(r)$ on the spherical coordinate angles $\theta$ and $\varphi$, the continuity eq. S2 takes the form:

$$\frac{d}{dr}\left(r^2 \frac{dC_i}{dr}\right) = -\frac{G}{D_i} r^2 \tag{S3}$$

By integrating the eq. S3 we get:

$$r^2 \frac{dC_i}{dr} = -\frac{G}{D}\frac{r^3}{3} + c_1, \tag{S4}$$

where the integration constant $c_1$ is related to the flow from the centre of the sphere as concentration gradient of iodine interstitials multiplied by the diffusion coefficient represents according to the Fick´s Law the diffusion current of iodine interstitials $J_{int}$. Since there is no

additional source of charged deep defects in the centre of the sphere, the integration constant $c_1$ must be zero and equation can be simplified to the form:

$$J_{int}(r) = -D_i \frac{dC_i}{dr} = \frac{Gr}{3}. \quad \text{(S5)}$$

The second integration of eq. S5 leads to the form:

$$C_i(r) = -\frac{Gr^2}{6D_i} + c_2, \quad \text{(S6)}$$

where the value of integration constant $c_2$ is given by the boundary condition, which considers that the concentration $C_i(R)$ has a defined value on the surface: $C_i(R)$ = constant. By setting the value of $c_2$ so that the dependence of concentration on the coordinate $r$ in eq. S6 disappears, we get:

$$C_i(r) = C_i(R) + G\frac{R^2 - r^2}{6D_i}. \quad \text{(S7)}$$

The simplified model derived above does not describe the formation of phase 2 as it does not consider the contribution of diffusion of iodine vacancies. For a detailed description of phases 1 and 2, a more detailed theoretical analysis is necessary.

References:


1 J. Holovský, S. De Wolf, J. Werner, Z. Remeš, M. Müller, N. Neykova, M. Ledinský, L. Černá, P. Hrzina, P. Löper, B. Niesen and C. Ballif, *J. Phys. Chem. Lett.*, 2017, **8**, 838–843.

2 E. T. Hoke, D. J. Slotcavage, E. R. Dohner, A. R. Bowring, H. I. Karunadasa and M. D. McGehee, *Chem. Sci.*, 2015, **6**, 613–617.

3 S. G. Motti, D. Meggiolaro, A. J. Barker, E. Mosconi, C. A. R. Perini, J. M. Ball, M. Gandini, M. Kim, F. De Angelis and A. Petrozza, *Nat. Photonics*, 2019, **13**, 532–539.

4 C. Yu, *J. phys. Energy*, 2019, **1**, 30.

5 M. C. Brennan, S. Draguta, P. V. Kamat and M. Kuno, *ACS Energy Lett.*, 2018, **3**, 204–213.

6 M. Hu, C. Bi, Y. Yuan, Y. Bai and J. Huang, *Adv. Sci.*, 2015, **3**, 6–11.

7 J. Barrier, R. E. Beal, A. Gold-Parker, J. A. Vigil, E. Wolf, L. Waquier, N. J. Weadock, Z. Zhang, L. T. Schelhas, A. F. Nogueira, M. D. McGehee and M. F. Toney, *Energy Environ. Sci.*, 2021, **14**, 6394–6405.

8 D. P. McMeekin, G. Sadoughi, W. Rehman, G. E. Eperon, M. Saliba, M. T. Hörantner, A. Haghighirad, N. Sakai, L. Korte, B. Rech, M. B. Johnston, L. M. Herz and H. J. Snaith, *Science (80-. ).*, 2016, **351**, 151–155.

9 C. Li, A. Guerrero, S. Huettner and J. Bisquert, *Nat. Commun.*, 2018, **9**, 8.

10 A. Senocrate, I. Moudrakovski, G. Y. Kim, T. Y. Yang, G. Gregori, M. Grätzel and J. Maier, *Angew. Chemie - Int. Ed.*, 2017, **56**, 7755–7759.